EITN90 Radar and Remote Sensing Lecture 3: Propagation Effects and Mechanisms

Daniel Sjöberg

Department of Electrical and Information Technology

Outline

Learning outcomes of this lecture

In this lecture we will

- ▶ Get an overview of propagation phenomena.
- ▶ See how they can be quantified using the propagation factor.
- ▶ Learn about the basic structure of the atmosphere and how it affects electromagnetic waves.
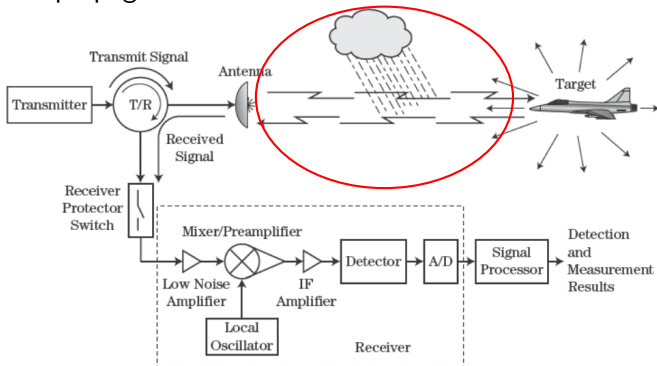- ▶ See the basics of diffraction phenomena and multipath propagation.

FIGURE 1-1 ■ Major elements of the radar transmission/ reception process.

Outline

Propagation factor

Propagation effects in addition to free space are modeled by the complex voltage propagation factor F_v

$$E_0' = F_v E_0 = (F e^{\mathrm{j}\phi_F}) E_0$$

where E_0' is the one-way received electric field strength, and E_0 is the corresponding field strength when only free space effects are considered. When N effects are considered, we have

$$F_v = F_{v1} F_{v2} \cdots F_{vN} = \underbrace{F_1 F_2 \cdots F_N}_{= \, F, \text{ amplitude}} \cdot \exp[\mathrm{j} \underbrace{(\phi_1 + \phi_2 + \cdots + \phi_N)}_{= \, \phi_F, \text{ phase}}]$$

In terms of power we need to consider

$$|F_v|^2 = F^2 = F_1^2 F_2^2 \cdots F_N^2$$

and the two-way propagation in the radar range equation implies

$$P_{\mathrm{r}} = \frac{P_{\mathrm{t}} G^2 \lambda^2 \sigma}{(4\pi)^3 R^4} F^4$$

Refractive index

The complex voltage propagation factor for a plane wave is

$$F_v = e^{-jnkr}$$

where $k = 2\pi f/c = \omega/c$ is the wave number in free space, r is the propagation distance, and n is the refractive index. This is usually complex-valued, $n = n' - jn''$, which implies

$$F_v = e^{-j(n'-jn'')kr} = e^{-jn'kr}e^{-n''kr}$$

This demonstrates that there is an exponential attenuation related to the imaginary part n'' of the refractive index, due to losses in the material. This will later be quantified in the attenuation coefficient α.

Line-of-sight and shadow regions

A target is in the line-of-sight (LOS) region if a straight line can be drawn to it from the transmitter without passing an obstacle.

FIGURE 4-2 ■
Regions defined by the LOS propagation path near the earth's surface.
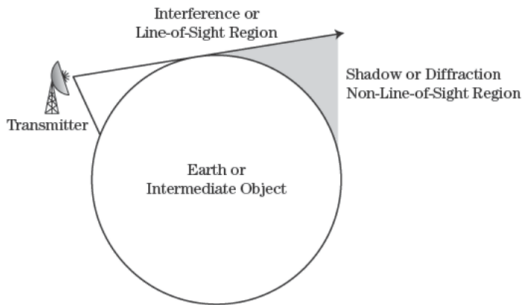
There can still be interaction with targets in the shadow region, due to refraction and diffraction effects. However, this is usually significantly weaker than LOS.

The atmosphere

The layered structure of the atmosphere can significantly affect the propagation of electromagnetics waves.
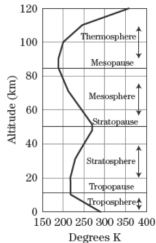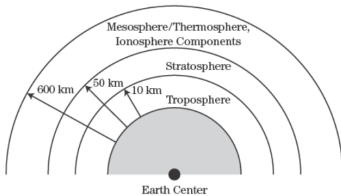

FIGURE 4-3 ■
Rays propagating through atmospheric regions. (From Eaves et al. [2] and Bogush [3]. With permission.)

- *Troposphere*: 4/5 of atmosphere mass, most weather processes (and water vapor) occur here.

- *Stratosphere*: little water, little weather, increasing temperature.

- *Mesosphere*: decreasing temperature, strong winds.

- *Thermosphere*: high temperature region.

- *Ionosphere*: atoms and molecules ionized by radiation.
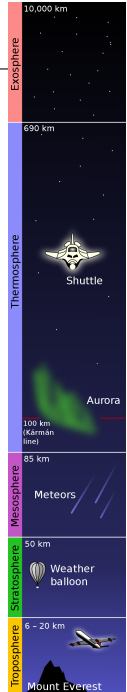
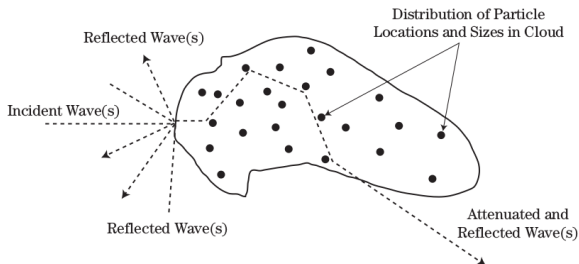# Outline

Attenuation by scattering and absorption

When a wave interacts with a cloud of particles, each particle can both scatter and absorb the wave, leading to attenuation.

FIGURE 4-4 ▪
Attenuation due to wave scattering and absorption by particulates.

Dense collections of particles, large compared to wavelength, attenuate more. The attenuation is characterized by the (two-way) attenuation coefficient α:

$$F^2 = 10^{\alpha L/2}, \quad F^2\,[\mathrm{dB}] = 10\frac{\alpha L}{2}, \quad [\alpha] = \mathrm{m}^{-1}$$

The two-way attenuation in dB is $F^4\,[\mathrm{dB}] = 10\alpha L$.

Heterogeneous atmosphere

For long range propagation, we need to consider combinations of several propagation regions.
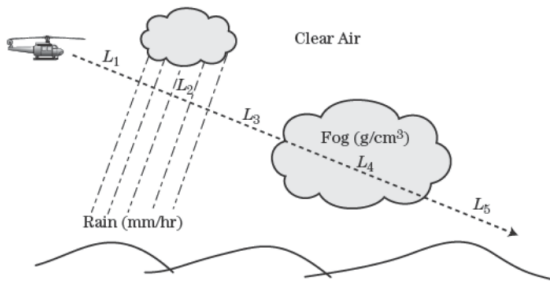

FIGURE 4-5 ■
Heterogeneous atmosphere impacts.

$$F^2 = 10^{\alpha_1 L_1/2} 10^{\alpha_2 L_2/2} \cdots 10^{\alpha_N L_N/2}$$

The attenuation can be due to atmospheric molecules as well as rain, fog, dust, and can vary strongly with time.

Typical attenuation coefficients

TABLE 4-1 ◾ Typical One-Way Attenuation Coefficients, α, for Some Selected Atmospherics at 10 GHz

Description	Attenuation Coefficient (dB/km)	Water Content (g/m^3)	Remarks
Clear air	0.01	7.5	Based on sea-level elevation, 42% relative humidity, and 20°C temperature
Dust	0.004	0.1	Based on sea-level elevation, 0 relative humidity, and 20°C temperature
Radiation fog	0.0688	0.1	Based on sea-level elevation, 100% relative humidity, and 20°C temperature
Fog oil (Engine smoke)	0.43	0.0001	Based on sea-level elevation, 0 relative humidity, and 20°C temperature
Rain (4 mm/hr) (10 mm/hr)	0.05 0.17	n/a[1]	Based on sea-level elevation, 100% relative humidity, and 20°C temperature
Snow (2 mm/hr)	0.0016	n/a[1]	Based on sea-level elevation, 100% relative humidity, and 0°C temperature
Special smokes and obscurants	8.6	0.001	Based on sea-level elevation, 0 relative humidity, and 20°C temperature

▸ Discussion question

Atmospheric gases and water vapor

FIGURE 4-6 ■ Attenuation coefficient due to atmospheric gases and water vapor. (a) Variation with temperature. (Courtesy of Bruce Wallace, MMW Concepts. With permission.) (b) Variation with altitude. (From P-N Designs, Inc. [6].)
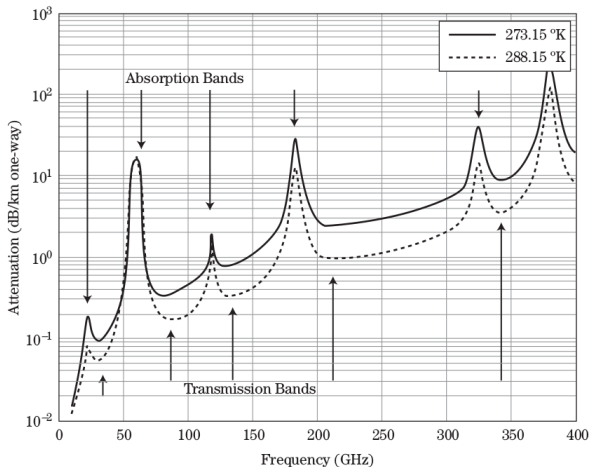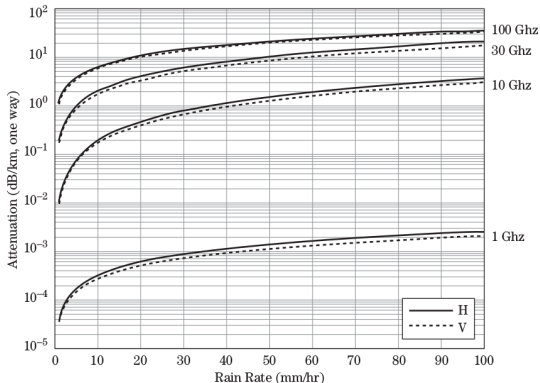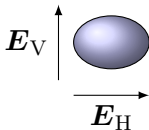
Peaks correspond to molecular resonances (rotational or vibrational), and may help isolating short-range systems. Long-range systems typically operate in regions of low attenuation.

Rain

Attenuation due to rain drops depend strongly on rain rate and frequency.

FIGURE 4-7 ▪
One-way attenuation versus rain rate at four frequencies.

The small difference between polarizations is due to the flattening of falling rain drops, becoming larger for horizontal polarization.
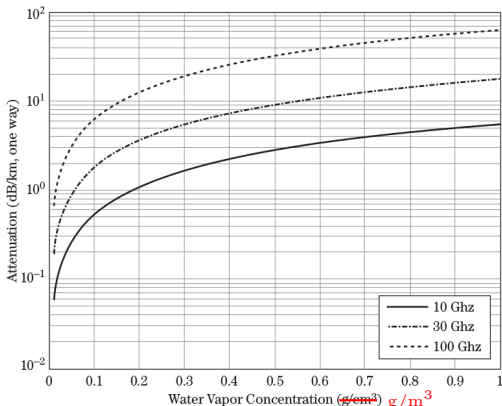
Fog

Using the formula (α in dB/km, M in $\mathrm{g/m^3}$, f in GHz, T in $°C$)

$$\alpha = M\left(-1.347 + 0.66\,f + \frac{11.152}{f} - 0.022\,T\right), \quad f > 5\,\mathrm{GHz}$$

the fog attenuation α as function of water vapor concentration M is as below. Data for different kinds of fog are found in Table 4-3.

FIGURE 4-8 ■
Attenuation at three frequencies for fog versus water concentration (fog type).

Attenuation (dB/km, one way)

Water Vapor Concentration (g/cm³) $\mathrm{g/m^3}$

TABLE 4-3 ■ Summary of Fog Types and Water Concentration Ranges

Type	Water Concentrations (g/m^3)	Remarks
Steam fog	0.1–1.0	Results from cold-air movements over warm water
Warm-front fog	0.1–1.0	Evaporation of warm rain falling through cold air, usually associated with the movement of a warm front, under certain humidity, conditions yields a supersaturated air mass at ground level
Radiation fog	0–0.1	Results from radiation cooling of the earth's surface below its dew level
Coastal and inland ground fog	0.1–1.0	Radiation fog of small heights
Valley fog	0.1–1.0	Radiation fog that forms in valleys
Advection fog	0–0.1	Formed by cool air passing over a colder surface
Up-slope fog	0.1–1.0	Results from the adiabatic cooling of air up-sloping terrain

Snow and hail

Frozen water in crystalline particles changes electromagnetic
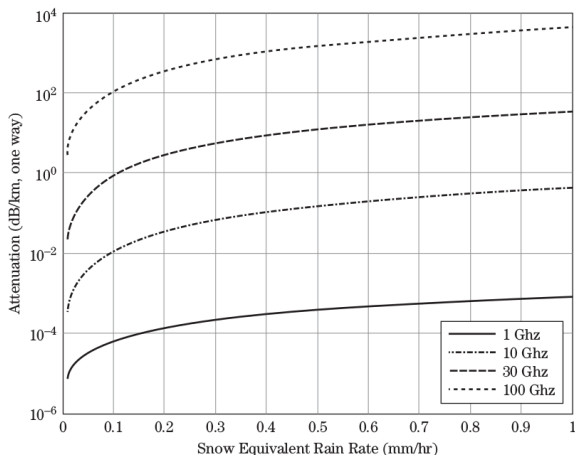properties. Larger effects than for rain at higher frequencies.

FIGURE 4-9 ■
Attenuation for snow
versus equivalent
rainfall rate at four
frequencies.

Similar characterizations apply to attenuation due to dust and
smoke.

Snow parameters

TABLE 4-4 ▪ Mean Diameters, Masses, and Fall Velocities of Snow Crystals

Snow Type	Diameter (mm)	Mass (mg)	Fall Velocity (cm/s)
Needle	1.53	0.004	50
Plane dendrite	3.26	0.043	31
Spatial dendrite	4.15	0.146	57
Powder snow	2.15	0.064	50
Rimed crystals	2.45	0.176	100
Graupel	2.13	0.80	180

Source: From Nakaya and Terada [9] (With permission).

$$\alpha = 0.00349 \frac{r_\mathrm{e}^{1.6}}{\lambda^4} + 0.00224 \frac{r_\mathrm{e}}{\lambda}$$

$$r_\mathrm{e} = Xv, \quad [X] = \mathrm{g/m^3}, \quad [v] = \mathrm{m/s}$$

For some nice examples of snow flake shapes:
http://snowcrystals.com/

Standard atmosphere

There are several models of "standard" atmosphere, for instance
US Standard Atmosphere and International Standard Atmosphere.
The models give a baseline for predictions. Typically, the refractive
index decreases as height increases, due to the thinning of the
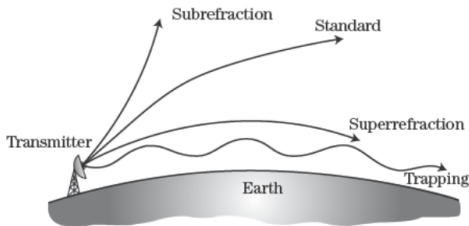atmosphere.

FIGURE 4-10 ■
Illustration of ray
bending for standard
and anomalous
refraction profiles.

When the real scenario leads to smaller or larger refraction than
the standard atmosphere, it is referred to as *anomalous refraction*,
further divided into *subrefraction*, *superrefraction*, and *trapping or
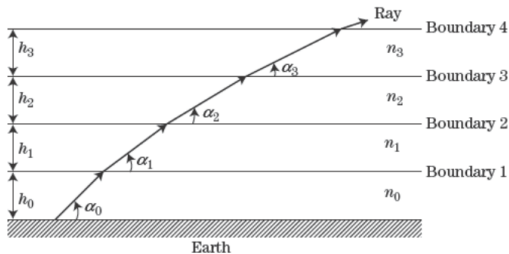ducting*.

Snell's law

FIGURE 4-11 ■
Path of a ray through a horizontally stratified atmosphere (troposphere).

Snell's law of refraction for a planar, layered structure, states that

$$n_0 \cos \alpha_0 = n_1 \cos \alpha_1 = n_2 \cos \alpha_2 = \cdots = n_i \cos \alpha_i$$

If the refractive index is decreasing, $n_0 > n_1 > n_2 \cdots$, then $\cos \alpha_i$ must be increasing, that is, α_i must be decreasing. Hence, the propagation direction of the wave is bent towards the earth (standard refraction).

Spherical form of Snell's law

FIGURE 4-12 ■
Path of a ray through a radially stratified atmosphere (troposphere).
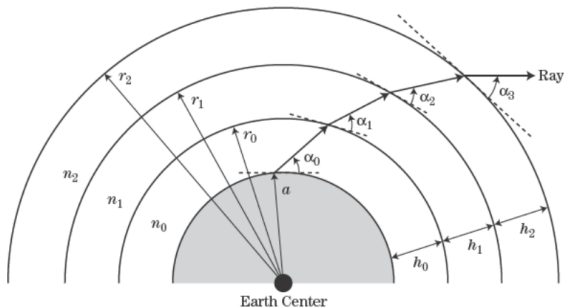
For a radial structure, Snell's law must be weighted with the radius,

$$n_0 r_0 \cos \alpha_0 = n_1 r_1 \cos \alpha_1 = n_2 r_2 \cos \alpha_2 = \cdots = n_i r_i \cos \alpha_i$$

This is a small correction, since the earth radius $a = 6\,371\,\mathrm{km}$ is much larger than the thickness of the atmosphere (around $100\,\mathrm{km}$). Hence, $r_1 \approx r_2 \approx \cdots \approx r_i$.

Angle and range estimation errors due to refraction

FIGURE 4-13 ■
Normal refraction
effects on target
location
(troposphere).
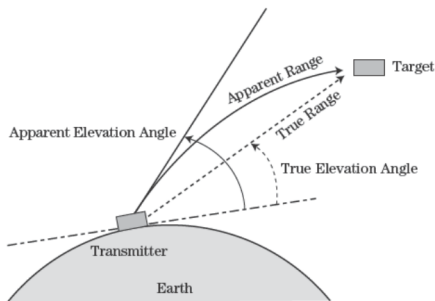
Elevation angle measured by radar appears larger than true
elevation.
Range measured by radar appears longer than true range.

▸ Discussion question

Angle estimation errors

FIGURE 4-14 ■
Normal refraction effects on target location—angle estimate, 0% humidity (troposphere).

Unfortunately, the book does not state the position of the target with respect to these curves. Largest error at high altitude and small grazing angle.
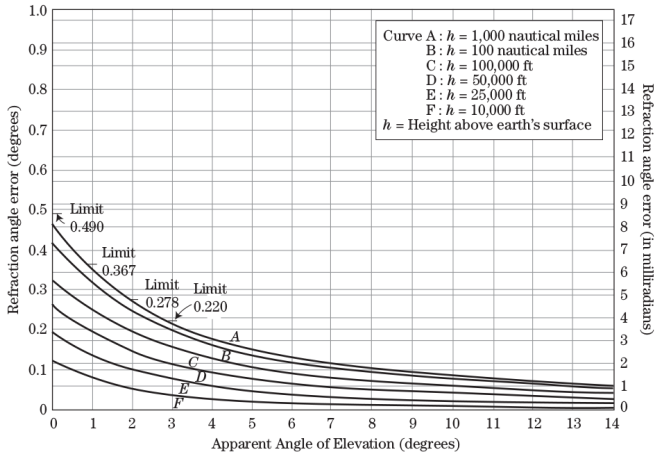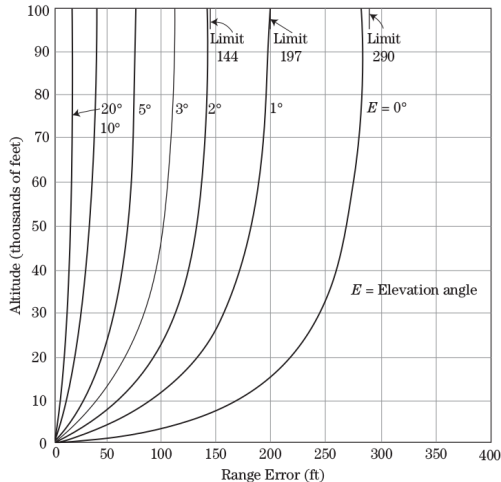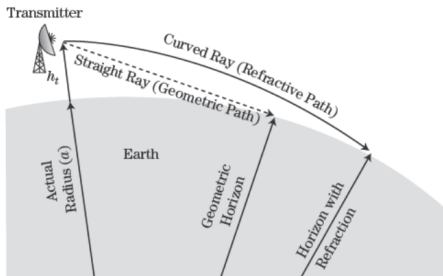
Range estimation errors

FIGURE 4-15 ■
Normal refraction effects on target location—range estimate, 0% humidity (troposphere).

Unfortunately, the book does not state the position of the target with respect to these curves. Largest error at high altitude and small grazing angle.

Effective earth model

FIGURE 4-16 ■
Increased range
to radar horizon due
to refraction.

The geometric radar horizon (assuming a spherical earth)

$$R_{\mathrm{h}} = \sqrt{2ah_{\mathrm{t}}}$$

The extended horizon R'_{h} due to refraction is given by the same formula if the effective earth radius a_{e} is introduced (calculated from $\frac{\mathrm{d}n}{\mathrm{d}h} = -3.9 \cdot 10^{-8}\,\mathrm{m}^{-1}$)

$$a \to a_{\mathrm{e}} \approx \frac{4}{3}a$$

Anomalous refraction

Propagation conditions differing from the standard model
($\frac{\mathrm{d}n}{\mathrm{d}h} \approx -4 \cdot 10^{-8} \, \mathrm{m}^{-1}$)

- *Subrefraction*: $\frac{\mathrm{d}n}{\mathrm{d}h} > 0$, rays bend upward.
- *Superrefraction*: $\frac{\mathrm{d}n}{\mathrm{d}h}$ more negative than standard atmosphere, rays bend more strongly downwards.
- *Ducting and trapping*: $\frac{\mathrm{d}n}{\mathrm{d}h} < -16 \cdot 10^{-8} \, \mathrm{m}^{-1}$, rays may be trapped in regions 10–20 m (sometimes up to 200 m) in height. This significantly extends the horizon.
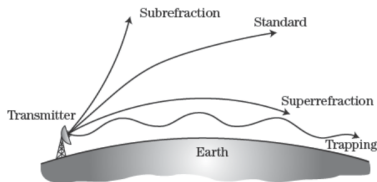

FIGURE 4-10 ■
Illustration of ray bending for standard and anomalous refraction profiles.

The ducting phenomenon is often caused by temperature and humidity effects, and can vary with time. Radar wave propagation can be very different at different times of day.

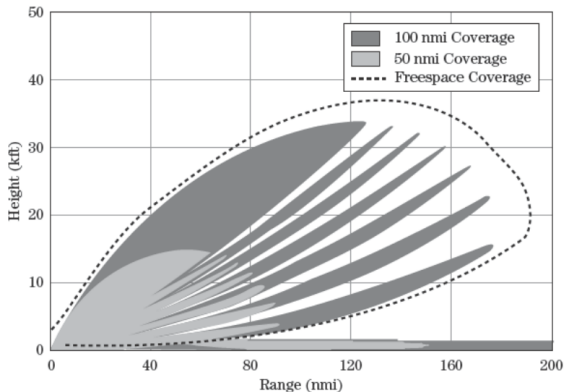# Effects of ducting on elevation coverage

FIGURE 4-20 ■ Illustration of ducting loss in radar elevation coverage.

The trapping of rays inside ducts depends on angle, and can produce significant distortion to the intended free space coverage. Requires good computer models to predict the behavior.

Outline

Turbulence

FIGURE 4-21 ■
Illustration of turbulence "pockets" in atmosphere.

Incident Wave

Turbulent Eddies
in the Atmosphere
with Differing Indices
of Refraction
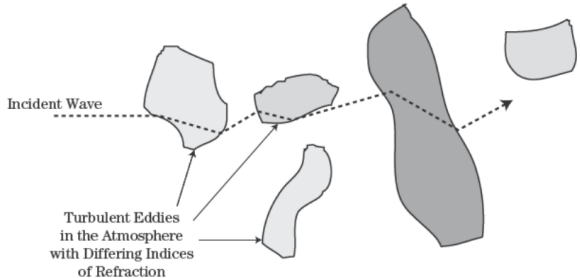
Atmospheric fluctuations, typically in clear, hot, humid weather. Mostly a problem at frequencies above $80\,\mathrm{GHz}$, fluctuations can be around 1–$2\,\mathrm{dB}$ in amplitude and 300 microradians in angle of arrival.

Ionosphere

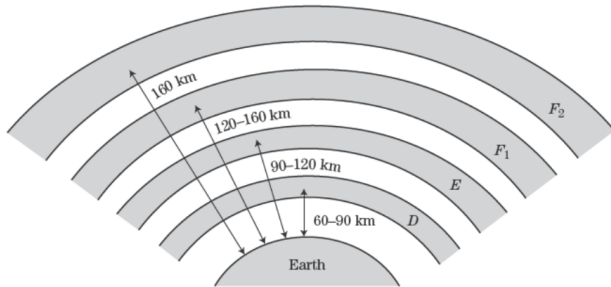**FIGURE 4-22** ■ Layers of the ionosphere (typical of noontime locations).

- ▶ D layer: exists only on daylight hours, bends and absorbs low frequency (3–7 MHz).
- ▶ E layer: similar characteristics to D, but higher altitude and exists at all hours.
- ▶ F1 layer: weaker than F2, blends into F2 at night.
- ▶ F2 layer: densest electron density, produced by UV. Bends waves below 30–50 MHz, strongest by day.

Ionosphere

The ionosphere is dispersive (frequency dependent) due to the free-moving electrons (electron density N_e, in $[\mathrm{electrons/m^3}]$)

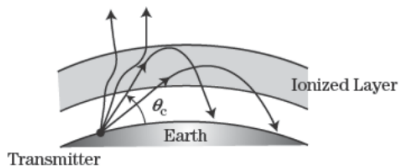$$n(f) = \sqrt{1 - \left(\frac{f_p}{f}\right)^2}, \quad f_p \approx 9\sqrt{N_e} \approx 9\,\mathrm{MHz}$$

FIGURE 4-23 ■
Bending of rays passing through an ionized layer at difference incidence angles.

With N_e increasing with height, n is decreasing if $f > f_p$. Using reflections in the ionosphere, a radar can see over the horizon. Requires low enough frequency, and low enough angle.

▸ Discussion question

Diffraction

Even though an obstacle is blocking the path, some power can be *diffracted* into the shadow zone.

FIGURE 4-24 ■
Illustration of virtual sources for diffraction around an obstacle.
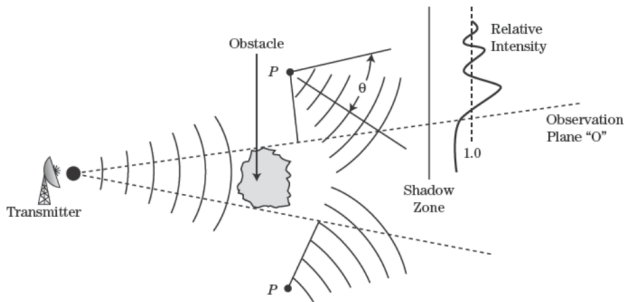
With a cylindrical object (long edge), the waves inside the shadow region are typically cylindrical waves (power decay as $1/R$):

$$F^2 = \frac{F^2(\theta)}{kR}$$

where $k = 2\pi/\lambda$ is the wave number.
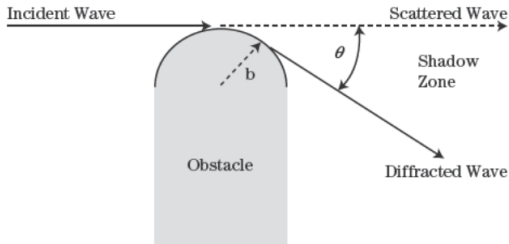
Knife-edge and rounded tip, formulas

FIGURE 4-25 ■
Geometry for
diffraction into
shadow zones.

Exact solutions can be found for simple geometries, depending on the radius of curvature b relative the wavelength λ, or $kb = 2\pi b/\lambda$:

$$F(\theta, kb = 0) = \frac{1}{2\sqrt{2\pi}}\left[\sec\left(\frac{\theta + \pi}{2}\right) + \csc\left(\frac{\theta + \pi}{2}\right)\right] \quad b < \lambda/50$$

$$F(\theta, kb) = (kb)^{1/3}\frac{C_0}{\sqrt{2}}\exp\left[-\tau_0(kb)^{1/3}\sin(\pi/3)\theta\right] \quad b > \lambda/50$$

Constants are $C_0 = 0.910719$ and $\tau_0 = 1.8557\exp(\pi/3) = 5.2881$. Strong dependence on curvature! (Some misprints in the book)

Knife-edge and rounded tip, graphs

FIGURE 4-26 ■
Local diffraction coefficient, F^2, behavior for two types of edges.

E^{inc} E^{diff} Visible Zone

Shadow Boundary

Shadow Zone

E^{inc} Scattered Wave

θ

E^{diff}

$b < \lambda/50$ $b > \lambda/50$
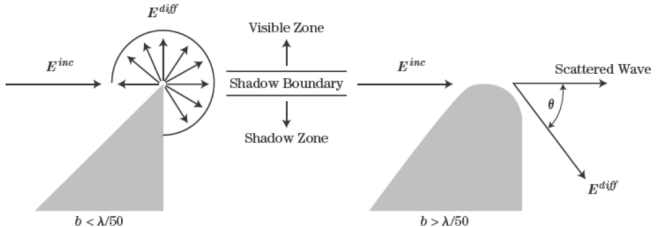
FIGURE 4-27 ■
Diffraction coefficient for rounded tip and knife edge versus shadow angle at 1 GHz.
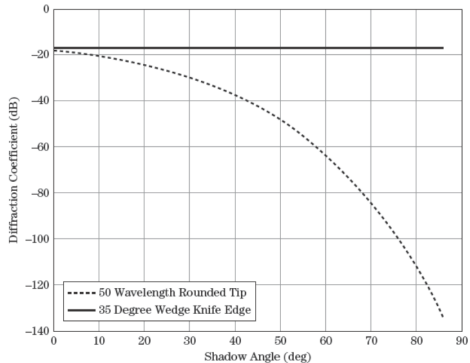
Diffraction Coefficient (dB)

- - - 50 Wavelength Rounded Tip
——— 35 Degree Wedge Knife Edge

Shadow Angle (deg)

Outline
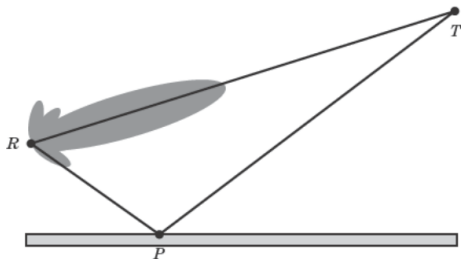
Multipath

FIGURE 4-28 ▪
Illustration of
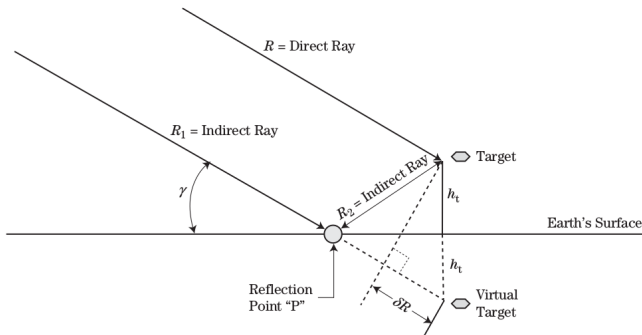multipath geometry
for ground reflection.

The electric field is propagated over four different paths:

- E_{dd}: path RTR (direct-direct, or DD).
- E_{di}: path RTPR (direct-indirect, or DI).
- E_{id}: path RPTR (indirect-direct, or ID).
- E_{ii}: path RPTPR (indirect-indirect, or II).

All the possibilities need to be added to find the total field.

Multipath

FIGURE 4-29 ■
Simplified multipath geometry for flat Earth and the virtual target.

R = Direct Ray

R_1 = Indirect Ray

R_2 = Indirect Ray

Target

h_t

Earth's Surface

Reflection Point "P"

h_t

δR

Virtual Target

γ

Using the reflection coefficient Γ, the one-way and two-way propagation factors are

$$F^2 = |1 + \Gamma \mathrm{e}^{-\mathrm{j}k\delta R}|^2$$
$$F^4 = |1 + 2\Gamma \mathrm{e}^{-\mathrm{j}k\delta R} + (\Gamma \mathrm{e}^{-2\mathrm{j}k\delta R})^2|^2$$

The book uses only $\cos(k\delta R)$, but ends up with correct results, for instance $F^2_{\max} = 6\,\mathrm{dB}$ and $F^4_{\max} = 12\,\mathrm{dB}$.

Coherent summation
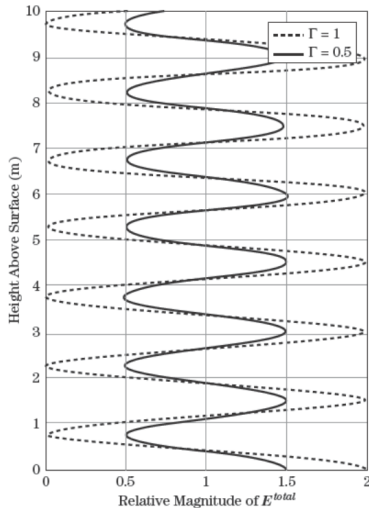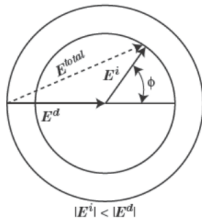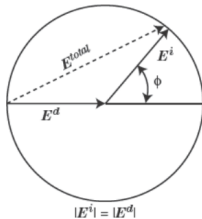
FIGURE 4-30 ■
Coherent summation
of direct and indirect
ray interference
pattern versus
observer height
above ground plane
(10 GHz, $h_a = 1$ m,
$d = 100$ m).

Depth of oscillation depends on amplitude of reflection coefficient.

Multipath signal lobing, one-way
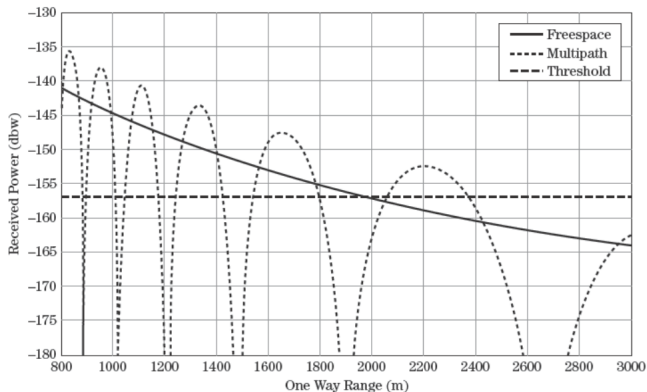
FIGURE 4-31 ■
Multipath signal
lobing versus free
space for one-way
geometry and $\Gamma = 1$.

Receiver height 10 m, frequency 10 GHz. Note that multipath
propagation can extend maximum range (signal above threshold).

The reflecting surface
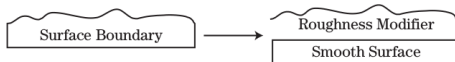
FIGURE 4-33 ■ Complex surface boundary decomposed into smooth and roughness factors.

The roughness of the surface (compared to wavelength) needs to be taken into account. Relative permittivity ϵ_r, conductivity σ_+, rms roughness σ_h, rms slope β_0. Spatial correlation is $T = \frac{2\sigma_h}{\tan\beta_0}$.

TABLE 4-5 ■ Surface Electrical and Physical Parameters at MMW ($\mu = 1$)

Surface Type	ε_r	σ_+ (mho/m)	σ_h (m)	β_0 (rad)
Mowed grass	10	0.001	0.01	0.1
Tall grass	10	0.001	0.1	0.2
Gravel	4	0.001	0.02	0.3
Asphalt	6	0.001	0.0004	0.36
Brush	4	0.001	0.5	0.1
Snow	2.5	0.001	0.003	0.25
Desert	2.5	0.001	0.003	0.05
Trees	1.5	0.001	1.5	0.2
Sea water	80	4	*	*
Fresh water	67	0.1	*	*

Multipath reflection coefficient

The multipath reflection coefficient

$$\Gamma = \Gamma_0 D(\rho_\mathrm{s} + \rho_\mathrm{d})$$

has several different contributions:

- Γ_0: Fresnel reflection coefficient of smooth earth surface.
- D: spherical earth divergence factor.
- ρ_s: specular roughness modifier.
- ρ_d: diffuse roughness modifier.

These are described shortly in the following.

Fresnel coefficients, smooth surface

At a flat interface between two materials, $(\epsilon_{rc1}, \mu_{rc1})$ and $(\epsilon_{rc2}, \mu_{rc2})$, the reflection coefficient of a plane wave incident from material 1 at grazing angle γ can be explicitly calculated,

$$\Gamma_0^{\mathrm{VV}} = \frac{\frac{\epsilon_{rc2}}{\epsilon_{rc1}} \sin \gamma - \sqrt{\frac{\epsilon_{rc2}\mu_{rc2}}{\epsilon_{rc1}\mu_{rc1}} - \cos^2 \gamma}}{\frac{\epsilon_{rc2}}{\epsilon_{rc1}} \sin \gamma + \sqrt{\frac{\epsilon_{rc2}\mu_{rc2}}{\epsilon_{rc1}\mu_{rc1}} - \cos^2 \gamma}}$$

$$\Gamma_0^{\mathrm{HH}} = \frac{\frac{\mu_{rc2}}{\mu_{rc1}} \sin \gamma - \sqrt{\frac{\epsilon_{rc2}\mu_{rc2}}{\epsilon_{rc1}\mu_{rc1}} - \cos^2 \gamma}}{\frac{\mu_{rc2}}{\mu_{rc1}} \sin \gamma + \sqrt{\frac{\epsilon_{rc2}\mu_{rc2}}{\epsilon_{rc1}\mu_{rc1}} - \cos^2 \gamma}}$$
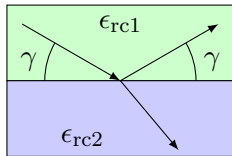

$\epsilon_{rc1}, \mu_{rc1}$

γ γ
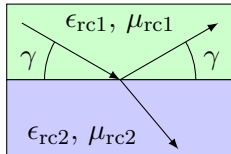
$\epsilon_{rc2}, \mu_{rc2}$

As $\gamma \to 0$, we have $\Gamma_0^{\mathrm{VV,HH}} \to -1$, that is, at small grazing angles there is complete reflection.

Fresnel coefficients, smooth surface

At a flat interface between two materials, $(\epsilon_{\mathrm{rc}1}, \mu_{\mathrm{rc}1})$ and $(\epsilon_{\mathrm{rc}2}, \mu_{\mathrm{rc}2})$, the reflection coefficient of a plane wave incident from material 1 at grazing angle γ can be explicitly calculated,

$$\Gamma_0^{\mathrm{VV}} = \frac{\frac{\epsilon_{\mathrm{rc}2}}{\epsilon_{\mathrm{rc}1}} \sin\gamma - \sqrt{\frac{\epsilon_{\mathrm{rc}2}}{\epsilon_{\mathrm{rc}1}} - \cos^2\gamma}}{\frac{\epsilon_{\mathrm{rc}2}}{\epsilon_{\mathrm{rc}1}} \sin\gamma + \sqrt{\frac{\epsilon_{\mathrm{rc}2}}{\epsilon_{\mathrm{rc}1}} - \cos^2\gamma}}$$

$$\Gamma_0^{\mathrm{HH}} = \frac{\sin\gamma - \sqrt{\frac{\epsilon_{\mathrm{rc}2}}{\epsilon_{\mathrm{rc}1}} - \cos^2\gamma}}{\sin\gamma + \sqrt{\frac{\epsilon_{\mathrm{rc}2}}{\epsilon_{\mathrm{rc}1}} - \cos^2\gamma}}$$

$\mu_{\mathrm{rc}1} = \mu_{\mathrm{rc}2} = 1$

As $\gamma \to 0$, we have $\Gamma_0^{\mathrm{VV,HH}} \to -1$, that is, at small grazing angles there is complete reflection.

Most often, the materials are non-magnetic ($\mu_{\mathrm{rc}1} = \mu_{\mathrm{rc}2} = 1$), and the complex permittivity can be written $\epsilon_{\mathrm{rc}}(\omega) = \epsilon_{\mathrm{r}} + \sigma_+/(\mathrm{j}\omega)$. (Formulas in the book apply only to $\mu_{\mathrm{rc}1} = \mu_{\mathrm{rc}2}$)
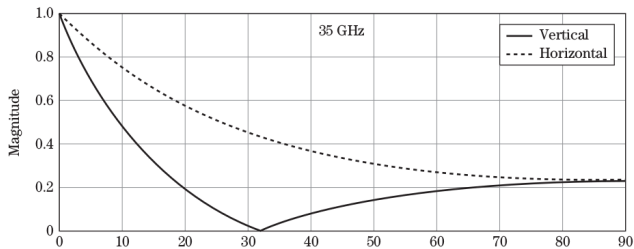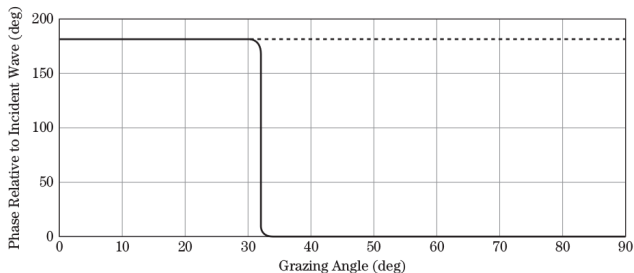
Fresnel coefficients, example

FIGURE 4-34 ▪
Fresnel reflection coefficient (magnitude and relative phase) for a desert surface.

$\epsilon_{rc1} = \mu_{rc1} = \mu_{rc2} = 1$, $\epsilon_{rc2} = 2.5$.

Critical angle, Brewster angle

▶ For a wave coming from a denser medium to thinner ($|\frac{\epsilon_{rc2}}{\epsilon_{rc1}}| < 1$), there is total reflection ($|\Gamma| = 1$) if the grazing angle $\gamma < \gamma_c$. The critical angle is $\gamma_c = \arccos(\sqrt{\epsilon_{rc2}/\epsilon_{rc1}})$ (or $\theta_c = \arcsin(\sqrt{\epsilon_{rc2}/\epsilon_{rc1}})$ in terms of angle to the normal). This explains how waves can be reflected in the ionosphere.

▶ For a vertically polarized wave, there is zero reflection at the Brewster angle $\gamma_B = \arctan(\sqrt{\epsilon_{rc1}/\epsilon_{rc2}})$, whereas the horizontally polarized wave is significantly reflected.
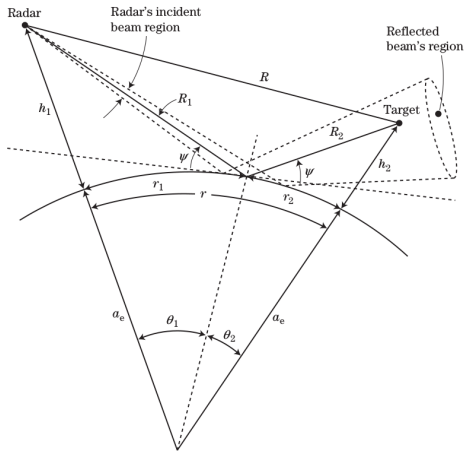
Divergence factor

FIGURE 4-36 ▪
Geometry for reflections from a spherical, smooth earth.

$$D \approx \left[1 + \frac{2r_1^2(r - r_1)}{a_\mathrm{e} r (h_1 - (r_1^2/2a_\mathrm{e}))} \right]^{-1/2}$$

Important at long ranges, beyond the horizon. Otherwise, $D \approx 1$.

Surface roughness

FIGURE 4-37 ■
Illustration of specular to diffuse scattering transitions with increasing surface roughness.
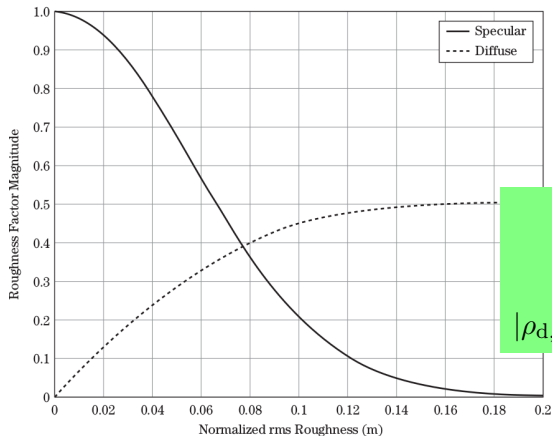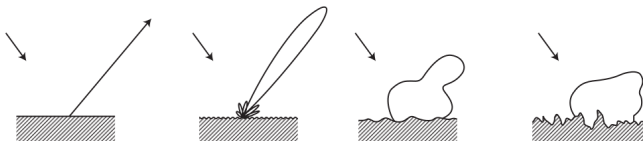

FIGURE 4-38 ■
Specular and diffuse roughness factor transition versus normalized surface rms roughness.

$$\sigma_h' = \frac{\sigma_h}{\lambda} \sin \gamma$$

$$|\rho_s| = \exp[-(4\pi\sigma_h')^2]$$

$$|\rho_{d,\text{limit}}| = 0.5\sqrt{1 - |\rho_s|}$$

A word of caution

The end of Section 4.9.3 becomes quite technical, with much new terminology. Do not dive too deeply into this if you find it confusing.

Outline

Wave propagation in a material

An electromagnetic wave propagates in a material with the factor

$$e^{-jk_c x} = e^{-\alpha x} e^{-j\beta x}, \quad k_c = \beta - j\alpha = \frac{\omega}{c} n_c, \quad n_c = \sqrt{\epsilon_{rc} \mu_{rc}}$$

The complex permittivity $\epsilon_c = \epsilon' - j\epsilon''$ has a typical frequency dependence as below (ϵ' typically decreasing with frequency):
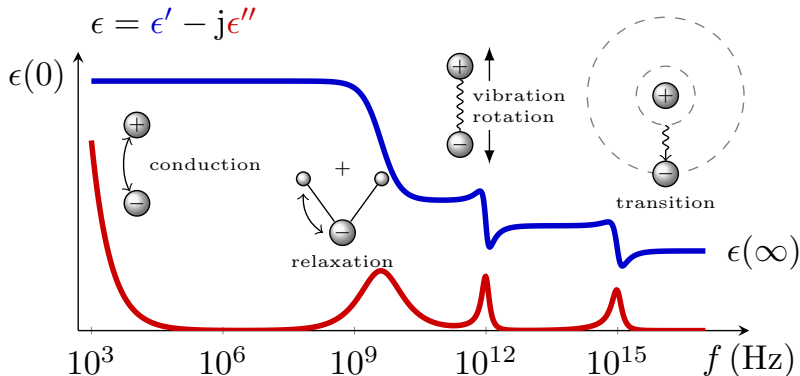
Skin depth

Electromagnetic waves propagating in a lossy medium attenuate as $\mathrm{e}^{-x/\delta}$, where $\delta = 1/\alpha$ is the skin depth. For good conductors

$$\delta = \sqrt{\frac{2}{\omega\mu\sigma_+}} = \sqrt{\frac{1}{\pi f \mu \sigma_+}}$$
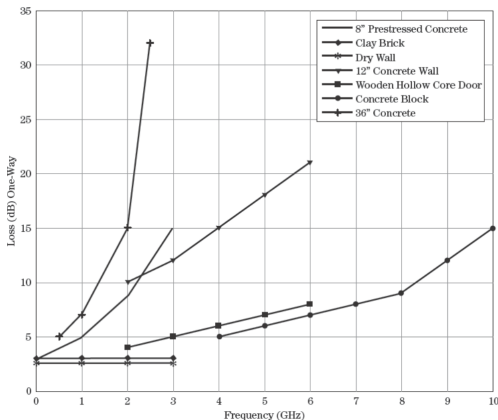

FIGURE 4-43 ≡
Radar wave
penetration through
some standard
materials.

Propagation delay

In addition to attenuation, material introduce delay due to reduced phase velocity, $v_{\mathrm{p}} = c/\operatorname{Re}(n_{\mathrm{c}})$. This is a source of errors in range estimation.

FIGURE 4-44 ■
Radar wave range delay through boundary materials with three refractive indexes.

Outline

Conclusions

Propagation in addition to free space is related to
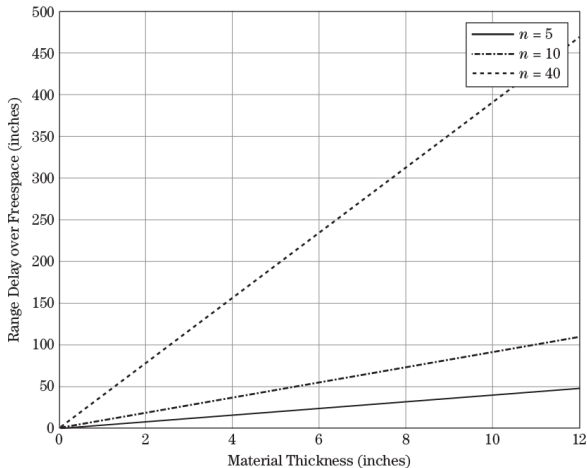
- ▶ Atmospheric attenuation due to scattering and absorption in molecules and particles; rain, fog, snow, dust etc.

- ▶ Refraction due to the layered structure of the atmosphere, gradient of refractive index.

- ▶ Turbulence, dispersive effects in ionosphere, diffraction at edges.

- ▶ Multipath propagation and interference can significantly modify the received power.

Some left-out topics

See the book for suggestions on further reading on the following topics:

- Atmospheric emission
- Surface wave propagation
- Ground-penetrating radar
- Atmospheric turbulence sensing
- Trans-ionospheric propagation

Why does clear air attenuate more than dust?

Discussion

Why does clear air attenuate more than dust?

Answer:

- ▶ Due to the higher humidity.

◂ Go back

When is the error in apparent range and elevation angle greatest:
at small or large elevation angles?

Discussion

When is the error in apparent range and elevation angle greatest: at small or large elevation angles?

Answer:

- ► Small.

Discussion

When is the error in apparent range and elevation angle greatest: at small or large elevation angles?

Answer:

► Small.

Think of the limiting case of a wave propagating radially from the earth surface. This is not refracted at all, since it travels at normal incidence to the layers.

‹ Go back

What happens when $f < f_{\mathrm{p}}$ in a plasma (where the refractive index is $n(f) = \sqrt{1 - (f_{\mathrm{p}}/f)^2}$ and the propagation factor is $\mathrm{e}^{-\mathrm{j}nk_0d}$)?

‹ Go back

Discussion

What happens when $f < f_{\mathrm{p}}$ in a plasma (where the refractive index is $n(f) = \sqrt{1 - (f_{\mathrm{p}}/f)^2}$ and the propagation factor is $\mathrm{e}^{-\mathrm{j}nk_0 d}$)?

Answer:

▶ The refractive index becomes imaginary, $n = -\mathrm{j}|n|$. This implies propagation factor $\mathrm{e}^{-\mathrm{j}nk_0 d} = \mathrm{e}^{-|n|k_0 d}$, that is, exponential attenuation.

◀ Go back

Discussion

What happens when $f < f_\mathrm{p}$ in a plasma (where the refractive index is $n(f) = \sqrt{1 - (f_\mathrm{p}/f)^2}$ and the propagation factor is $\mathrm{e}^{-\mathrm{j}nk_0d}$)?

Answer:

- The refractive index becomes imaginary, $n = -\mathrm{j}|n|$. This implies propagation factor $\mathrm{e}^{-\mathrm{j}nk_0d} = \mathrm{e}^{-|n|k_0d}$, that is, exponential attenuation.

Sidetrack: there is a choice to be made in taking the square root of a negative number, $\sqrt{-1} = \pm\mathrm{j}$. Our choice $\sqrt{-1} = -\mathrm{j}$ is dictated by following a more detailed model of the plasma (including small losses), where it can be seen that we really have $\sqrt{-1 - \mathrm{j}\delta} = -\mathrm{j} + \delta/2 + \mathrm{O}(\delta^2) \to -\mathrm{j}$ as $\delta \to 0+$.

Discussion

Why are microwave ovens run at $2.45\,\mathrm{GHz}$?

Discussion

Why are microwave ovens run at $2.45\,\mathrm{GHz}$?

Answer:
▶ This is close to the maximum peak of losses in liquid water, but not exactly on top. This is because we want the waves to heat the interior as well as the surface of the food.

$\epsilon = \epsilon' - \mathrm{j}\epsilon''$ Water permittivity at $25°\,\mathrm{C}$